UNDERSTANDING INPUT TRANSFORMATION-BASED ATTACKS VIA TARGET FUNCTION SPACE EXPANSION

Anonymous authors
Paper under double-blind review

ABSTRACT

Research on transfer-based adversarial attacks provides critical insights into distinctions among Deep Neural Networks (DNNs), revealing their vulnerabilities when exposed to unseen noise. Among these transfer-based adversarial attacks, input transformation-based attacks are popular due to their simplicity and effectiveness. However, their mechanisms remain poorly understood, potentially hindering advancements in DNNs. This work explores the mechanism of the attacks, suggesting that 1) when trained with input transformations, models can improve transformation invariance by capturing diverse features from transformed inputs rather than transformation-invariant features. Therefore, given a surrogate model f_s trained with input transformations φ, adversarial attacks can leverage these transformations to expand the target function space $f_s \circ \varphi$, thereby effectively and rapidly improving adversarial transferability, as domain shifts are mitigated; 2) input transformation-based attacks enhance adversarial transferability by expanding the target function space. Such transformations effectively act as modifications to the target model, thereby improving attack robustness against diverse models; and 3) L2-normalization should be incorporated into the attack paradigm to mitigate gradient imbalance during adversarial example generation. This imbalance arises from domain shift variability induced by different transformations. Based on the findings, we design a simple transformation-based attack called SimAttack. It achieves a mean attack success rate of 95.4% on 12 models, and some of the generated examples are also effective against GPT 4.1.

1 INTRODUCTION

To identify the deficiencies of DNNs, researchers investigate the way to deceive a model by adding perturbations to inputs, which refers to an adversarial attack. Later, it reveals that these adversarial attacks can deceive another model while crafting noisy inputs for one model (i.e, surrogate models). Thus the transferability study of adversarial attacks has come into focus and many novel transfer-based attacks are proposed to improve the transferability of adversarial attacks, such as gradient-based methods (Goodfellow et al., 2014; Kurakin et al., 2018; Dong et al., 2018; Fang et al., 2024), input transformation-based methods (Xie et al., 2019; Zou et al., 2020; Lin et al., 2024; Zhu et al., 2024a; Guo et al., 2025), model-related methods (Zhang et al., 2023; Xiaosen et al., 2023; Wang et al., 2024b), ensemble-based methods (Liu et al., 2016; Chen et al., 2023a;b) and generation-based methods (Naseer et al., 2019; Zhu et al., 2024b).

Among these transfer-based adversarial attacks, input transformation-based attacks are popular due to their simplicity and effectiveness, and the update process for such attacks can be uniformly formulated as

$$x_t^{adv} = x_{t-1}^{adv} + \alpha \cdot sign(\sum_i \nabla_{x_{t-1}^{adv}} J(f_s(\varphi_i(x_{t-1}^{adv})), y)), \tag{1}$$

where x_t^{adv} denotes the adversarial example at the t-th iteration, and α is the step size. This parameter is typically set to ϵ/T (i.e., the perturbation budget ϵ divided by the total iterations T), ensuring the perturbation intensity remains within budget. The f_s represents the surrogate model, while φ_i denotes the i-th random transformation.

Here, inspired by the work Guo et al. (2025), we provide a more intuitive definition. Input transformation-based attacks leverage random transformation $\varphi(\cdot)$ to construct multiple composite functions $f_s(\varphi_i(\cdot))$ belonging to the function space $f_s \circ \varphi$, totaling I instances. The input x_{t-1}^{adv} is used to query these functions to obtain the updated adversarial example x_t^{adv}, which can enable the updated data x_t^{adv} to attack all the functions in the function space. This process can enhance adversarial transferability, allowing the adversarial example x_t^{adv} to effectively attack other models.

From the above definition, this transformation modifies the surrogate model, not the input data. Each transformation instance $\varphi_i(\cdot)$ can be viewed as a function $\varphi_i : R^{C\times H\times W} \rightarrow R^{C\times H\times W}$, and then all the compositions $f_s(\varphi_i(\cdot))$ can construct a function space. If the target models $f_{tar}(\cdot)$ reside in this function space, such attacks successfully transfer to them. We argue that input transformation-based attacks leveraging $\varphi(\cdot)$ can enhance model transformation invariance of adversarial examples by adopting transformations that bridge feature-capture gaps between surrogate and target models, thereby boosting adversarial transferability. The model transformation invariance refers to the fact that adversarial examples remain effective even when the target model undergoes a transformation.

However, if the surrogate model fails to extract meaningful features from these transformed data $\varphi_i(x_{t-1}^{adv})$, the resulting updates may become severely noisy. Consequently, if the transformed data $\varphi_i(x_t^{adv})$ resembles in-domain training data, adversarial attacks leveraging such transformations can generate effective perturbations. This efficacy stems from models' inherent strength in processing in-domain data. The Methodology section (i.e., Sec. 3) will investigate the effect of domain shift induced by data transformations and the feasibility of its mitigation.

Additionally, a critical concern emerges: if models learn transformation-invariant features, random transformations cannot expand the function space, thereby rendering the method ineffective. This limitation arises because capturing the same features before and after the transformation will result in identical example gradients before and after the transformation. Typically, transformations $\varphi(\cdot)$ are employed during training to enhance model transformation-invariance, defined as consistent outputs for original and transformed inputs. Intuitively, this is because models may capture transformation-invariant features. This issue will also be discussed in the Methodology section.

This study mainly investigates the aforementioned issues, with contributions summarized as follows:

- When trained with input transformations, models can improve transformation invariance by capturing diverse features from transformed inputs rather than transformation-invariant features. Consequently, given a surrogate model trained with input transformations, adversarial attacks can leverage these transformations to expand the target function space, thereby effectively and rapidly improving adversarial transferability, as models excel on in-domain data.
- Input transformation-based attacks enhance adversarial transferability by expanding the target function space. Such transformations effectively act as modifications to the target model, thereby improving attack robustness against diverse models.
- During adversarial example generation, varying domain shifts across different transformations can cause gradient imbalance and excessive noise. To address this, we introduce gradient normalization while employing a large set of random transformations.
- Based on these findings, we propose SimAttack, a simple yet effective transformation-based attack. This method leverages transformations used in surrogate model training along with other effective ones, incorporating gradient normalization to achieve state-of-the-art results in the experimental evaluations.

2 Related Work

This work mainly focuses on the mechanism interpretability of input transformation-based attacks, but also touches on mechanisms for model-related attacks and utilizes some ideas from gradient attribution. Therefore, in this section, we introduce these three types of related work.

Input Transformation-Based Attack. One of the most popular approaches is the input transformation-based attack due to its effectiveness and simplicity. The input transformation-based attack elaborates transformations to enhance adversarial transferability. DIM Xie et al. (2019) randomly resizes and adds padding to input examples to improve adversarial transferability. Consequently, DEM Zou et al. (2020) calculates the average gradient of several DIM's transformed images to further improve adversarial transferability. Then, many novel transformations are presented, which calculate the average gradient of the transformed images to improve adversarial transferability. For example, SSM Long et al. (2022) randomly scales images and adds noise in the frequency domain. SIA Wang et al. (2023) splits the image into blocks and applies various transformations to each block. DeCowA Lin et al. (2024) augments input examples via an elastic deformation to obtain rich local details of the augmented inputs. L2T Zhu et al. (2024a) optimizes the input-transformation trajectory along the adversarial iteration, achieving great performance. BSR Wang et al. (2024a) randomly shuffles and rotates the image blocks to generate adversarial examples with great adversarial transferability. OPS Guo et al. (2025) observes a mirroring relationship between model generalization and adversarial example transferability and uses transformation and random perturbations to generate adversarial examples. The mechanism underlying this approach is not well understood. To mitigate this, our work demonstrates that data transformation can help adversarial attacks avoid low-transferability perturbations by guiding adversarial examples to attack more models.

Model-Related Attack. This approach improves adversarial transferability by changing properties of surrogate models, such as data transformation and structural changes. SGM Wu et al. (2020) utilizes more gradients from the skip connections in the residual blocks. MTA Qin et al. (2023) trains a meta-surrogate model, whose adversarial examples can maximize the loss on a single or a set of pre-trained surrogate models. AGS Wang et al. (2024b) trains surrogate models with adversary-centric contrastive learning and adversarial invariant learning. VDC Wang et al. (2024a) adds virtual dense connections for dense gradient back-propagation in attention maps and MLP blocks, without altering the forward propagation. Our work investigates the role of input transformations.

Gradient-Based Feature Attribution. This approach delves into identifying the importance of input features to the model's output. CAM Zhou et al. (2016) identifies discriminative regions that the model uses to make a prediction through the linearly weighted summation of activation maps from the last convolution layer. Grad-Cam Selvaraju et al. (2017) introduces a general method that uses the gradients w.r.t. the activation map to measure the channel importance. Later, some novel methods Xu et al. (2020); Zhuo & Ge (2024) are proposed to improve performance by reducing noise, but the key idea remains unchanged. Our work uses feature attribution to demonstrate whether there are differences in the features captured by the model before and after data transformation.

3 METHODOLOGY

3.1 ROLE OF TRANSFORMATION IN MODEL TRAINING

Among previous transfer-based adversarial attacks, some methods Wu et al. (2020); Qin et al. (2023); Wang et al. (2024b;a), referred to as model-related attacks, enhance adversarial transferability by strategically modifying surrogate models. This demonstrates that the properties of surrogate models play a crucial role in adversarial example generation. Meanwhile, input transformations are widely used in model training to improve transformation invariance, implying they influence surrogate model characteristics. Then **what is the influence, and what difference do they make when using in input transformation-based attacks compared to other transformations?**

Typically, data transformations are considered to provide models with transformation-invariance. In other words, whether a model processes transformed data or original data, it can produce invariant outputs. Intuitively, this may arise from models capturing transformation-invariant features through data transformations. However, the results shown in Fig. 1 demonstrate that this is not true. As shown in Fig. 1, we utilize the feature attribution to show the difference between the captured features of original and transformed data and calculate the similarity between the results, which can be formulated as:

$$Cos(\nabla_x J(f_s(\varphi(x)), y), \nabla_x J(f_s(x), y)), \tag{2}$$

where $Cos(\cdot, \cdot)$ computes cosine similarity, and other symbols align with Eq. 1.

To investigate whether models can capture transformation-invariant features via data transformation, we train models on CIFAR-100 Krizhevsky et al. (2009) transformed by random rotation and resize-padding. We then compare gradient-based feature attribution maps between transformed and non-transformed inputs using Eq. 2. To show the influence of data transformations used in model training, beyond the transformation (i.e., rotation) employed during training, we introduce a transformation (i.e., block shuffle) unused in training for comparison. If models successfully capture

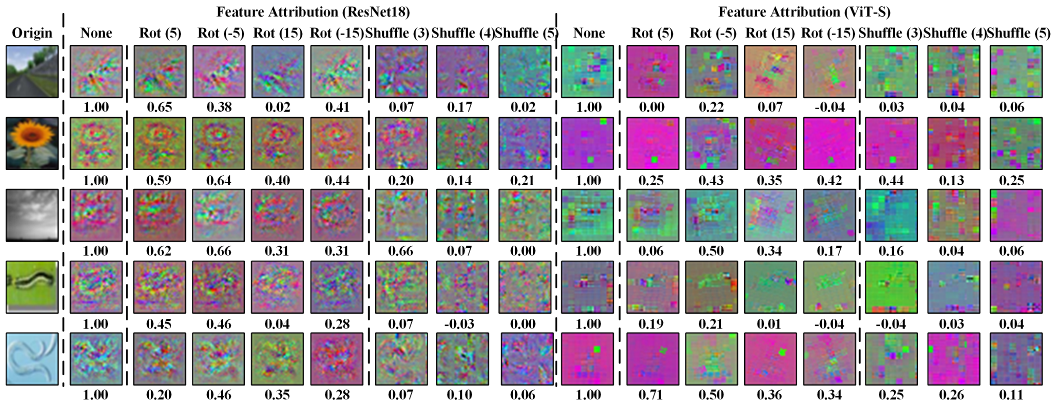

Figure 1: Similarity between gradients of inputs with and without transformation (i.e., the columns labeled "None" and others). Similarity can be calculated by Eq. 2. The used models are trained using data transformed by random rotation and resize-padding. The "None" column refers to inputs with no transformation, "Rot" to inputs with rotation, and "Shuffle" to inputs with block shuffle. Specifically, the "Rot (5)" indicates a rotation of 5 degrees, while "Shuffle (3)" indicates that inputs are split into several blocks and these blocks are randomly shuffled. The results suggest that although models can yield invariant outputs when processing transformed data, the models capture different features derived from the transformed data rather than invariant features.

transformation-invariant features, the feature attribution maps of the transformed and original data should be identical or highly similar. This can be formulated as

$$\nabla_x J(f_s(\varphi(x)), y) = \nabla_x J(f_s(x), y). \tag{3}$$

This invariance will lead to the degradation of input transformation-based attacks when utilizing transformations used in surrogate model training. The degradation can be formulated as

$$\begin{aligned} x_t^{adv} &= x_{t-1}^{adv} + \alpha \cdot sign(\sum_i \nabla_{x_{t-1}^{adv}} J(f_s(\varphi_i(x_{t-1}^{adv})), y)) \\ &= x_{t-1}^{adv} + \alpha \cdot sign(\nabla_{x_{t-1}^{adv}} J(f_s(x_{t-1}^{adv}), y)). \end{aligned} \tag{4}$$

However, the results in Fig. 1 demonstrate that regardless of whether a transformation was used in training, models produce different responses to the transformed inputs. This suggests that models cannot capture transformation-invariant features via data transformation. Instead, the models establish more projections $\varphi(x) \to y$. This supports that input transformation-based attacks do not degenerate into non-transformation-based attacks when utilizing the transformation used in surrogate model training. Therefore, we can utilize the transformation used in surrogate model training as the random transformation φ in the attack, guiding adversarial examples to target a set of functions $f_s(\varphi_i(\cdot))$ (belonging to a function space) instead of a single function $f_s(\cdot)$. Straightforwardly, this can improve the adversarial transferability of the adversarial examples while having little impact on the attack success rate against the surrogate model $f_s(\cdot)$, since the transformed data $\varphi_i(x)$ remains in-domain for the surrogate model $f_s(\cdot)$. To further demonstrate these points, we train surrogate models with and without transformations and then use the models to generate adversarial examples with and without the transformations. The results of these adversarial examples are shown in Fig. 2.

The results in Fig. 2 show that surrogate models trained with transformations can leverage the transformations to generate better adversarial examples superior to those generated without the transformations. This also supports that data transformation helps models establish more projections $\varphi(x) \to y$ rather than capturing transformation-invariant features. Also, the comparison of surrogate models with and without transformations reveals that models exhibiting better generalization capabilities typically generate more effective adversarial examples.

In summary, the role of data transformation is to help models capture different features from transformed data rather than capturing transformation-invariant features. Therefore, input transformation-based attacks can leverage the transformation used in surrogate model training as the random transformation φ in the attack, guiding adversarial examples to target a set of functions $f_s(\varphi_i(\cdot))$ to improve transferability.

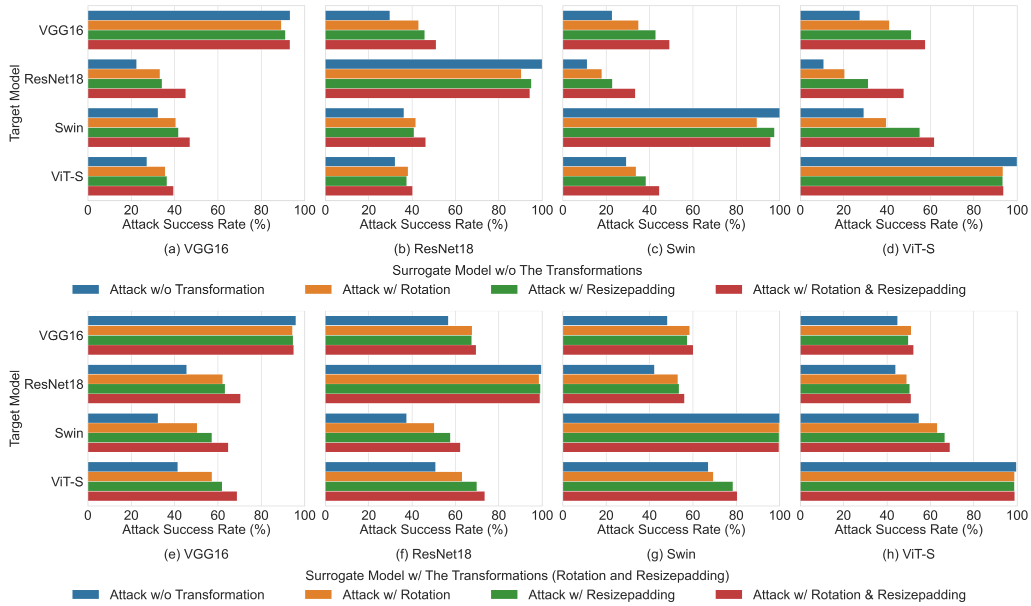

Figure 2: Attack success rate of input transformation-based attack with and without the data transformation used in surrogate model training. The surrogate models are trained on CIFAR-100, and the transformation number I of the attack is 100. We evaluate the performance on the data that can be classified correctly by all the models.

3.2 Mechanism of Input Transformation-Based Attacks

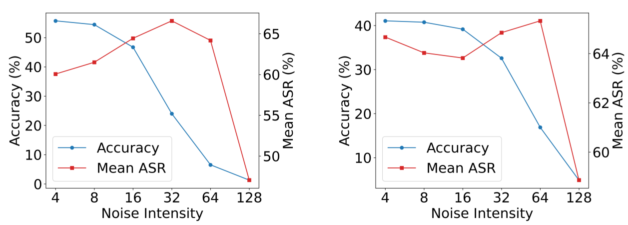

(a) ResNet18 (b) ViT-S

Figure 3: Accuracy of noisy inputs and mean attack success rate of adversarial attacks that employ random uniform noise as the transformation. The transformation number I is 100, with noise intensity defining the bounds of uniform sampling. We run 5 times and take the mean. This illustrates the trade-off between domain shift induced by data transformations $\varphi(\cdot)$ and the range of target function space $f_s(\varphi(\cdot))$.

The results in Fig. 2 show that input transformation-based attacks introduce the transformation (i.e., rotation and block shuffle) to improve adversarial transferability, even when surrogate models are trained without them. This suggests that, beyond the transformations used in surrogate model training, the attacks can introduce additional transformations to enhance transferability. However, this introduces a trade-off: while data transformations $\varphi(\cdot)$ expand the target function space $f_s \circ \varphi$, they simultaneously induce domain shifts that degrade the model. To further illustrate this clearly, we generate adversarial examples with noise of different intensities, and the results are presented in Fig. 3. We can expand the function space $f_s(\varphi(\cdot))$ by enhancing the bound of random noise, as a larger bound encompasses smaller variations. The domain shifts are demonstrated through the accuracy of images with varying noise intensities. As shown in Fig. 3, severe domain shift leads to model degradation. However, compared to downstream tasks, its impact on adversarial attacks is significantly less pronounced. This phenomenon may arise because the attack mechanism can leverage feature projections from any category, whereas the downstream task relies solely on projections corresponding to the correct category. Note that, as shown in Fig. 2, introducing such transformations into surrogate model training can mitigate the domain shift, but incurs higher hardware costs and increased time consumption.

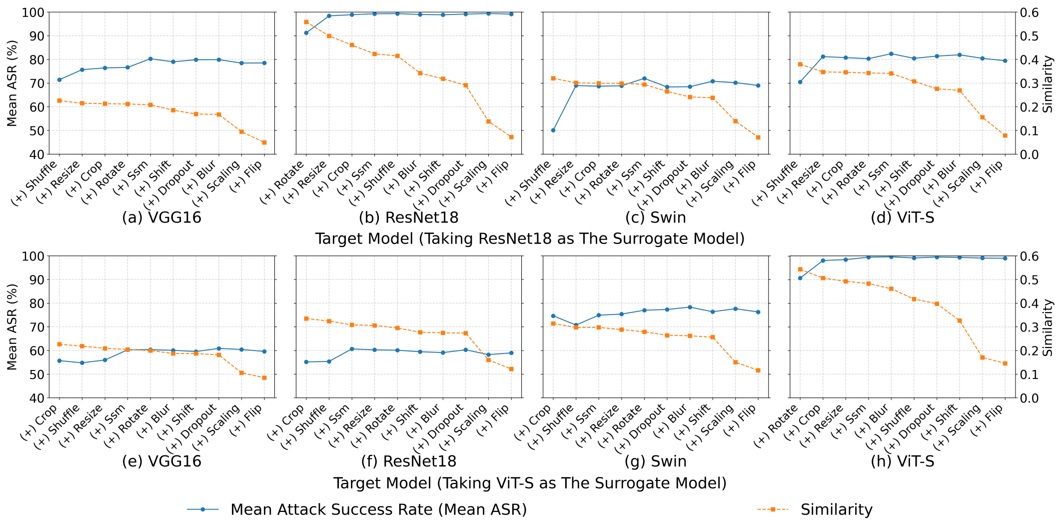

Figure 4: The similarity between adversarial examples generated through the approach in Eq. 5 and those produced using individual transformations. We then rank the transformations based on similarity and report the mean attack success rate for the ordered combination of these transformations. The similarity approximates each transformation's contribution. The transformations employed include block-shuffle Wang et al. (2024a), resize-padding Xie et al. (2019), random cropping, ssm Long et al. (2022) (which randomly scales images and adds noise in the frequency domain), random shift, dropout, Gaussian blurring, random scaling, and random flip. The models are trained on CIFAR-100 with rotation and resize-padding.

So far, we know that it is feasible to expand the function space through transformations that are not used in training. We next explore compensating for model differences through function space expansion centered on surrogate models. An ensemble attack-like task is introduced to generate adversarial examples, which can be formulated as

$$\frac{1}{I}\sum_{i} J(f_s(\varphi_i(x)), y) + J(f_{tar}(x), y), \tag{5}$$

where f_{tar} denotes the target model, and the φ_i represents a composite transformation sampled from a transformation set Ψ. We quantify the similarity between adversarial examples generated through the approach in Eq. 5 and those produced using individual transformations. The similarity approximates each transformation's contribution, with results visualized in Fig. 4. The results reveals that despite architectural differences among target models, transformation contribution rankings remain remarkably consistent, particularly for the least effective transformations. Although function space expansion via transformations exhibits some bias, transformations yielding limited function space expansion typically underperform across all target models.

3.3 Proposed Input Transformation-Based Attack

Based on our findings, we propose a simple transfer-based attack named SimAttack, as shown in Alg. 1. To maximize the function space, we randomly select several transformations from the transformation set Ψ as a composite transformation φ_i (Row 3 in Alg. 1), rather than serially combining all transformations or using other methods. Furthermore, we observe that domain shifts caused by different transformations may lead to gradient imbalances, as shown in Tab. 1. Specifically, gradients derived from transformations used during training tend to be smaller than those from other transformations. Therefore, inspired by optimizers Kingma & Ba (2014); Loshchilov & Hutter (2017), we introduce l_2-norm over each input as the normalization $Norm(\cdot)$ into our proposed attack (Row 4 in Alg. 1), thereby mitigating gradient imbalance.

Table 1: Gradients of inputs with different transformations. We average the results of 10,000 transformed data.

	Rotation	Resize-padding	Block Shuffle	Shift
ResNet18	0.0282	0.0207	0.0740	0.0830
ViT-S	0.0813	0.0793	0.1406	0.1427

As mentioned above, data transformation causes domain shifts, which in turn lead to increased noise in gradients. Increasing the number of random transformations mitigates noise, and we quantify this relationship in Fig. 5a and Fig. 5b. A single transformation may require more than 100 times to achieve optimal performance. Therefore, the transformation number may need to be set to several thousand to achieve optimal performance when using a number of transformations.

Algorithm 1 A simple transfer-based attack (SimAttack)

Input: an benign example x_0, adversarial example x_t^{adv}, perturbation budget ϵ, transformation set Ψ, step size α, iteration T, transformation number I.
Output: adversarial example x_T^{adv}.

1: Initialize $\alpha = \epsilon/T$, $x_0^{adv} = x_0$, $\overline{g_0} = 0$.
2: **for** $t = 1$ **to** T **do**
3: Sample I transformation compositions $\{\varphi_i\}_{i=0}^{I}$ from transformation set Ψ.
4: Update $g_t = \sum_i^I Norm(\nabla_{x_{t-1}^{adv}} J(f(\varphi_i(x_{t-1}^{adv})), y))$.
5: Update the momentum $\overline{g_t} = \overline{g_{t-1}} + \frac{g_t}{\|g_t\|_1}$.
6: Update the example $x_t^{adv} = clip(x_{t-1}^{adv} + \alpha \cdot sign(\overline{g_t}), 0, 1)$.
7: **end for**
8: **return** the adversarial example x_t^{adv}

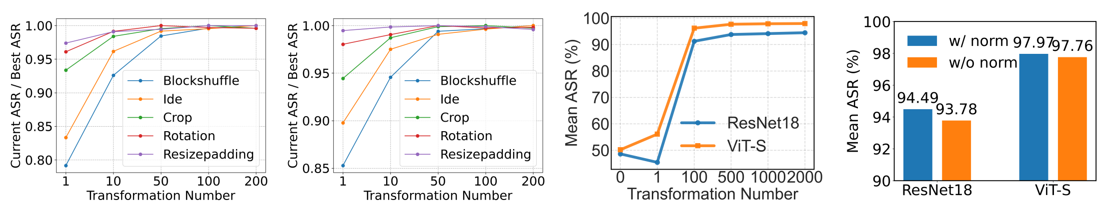

(a) ResNet18 (b) ViT-S (c) Transformation Number (d) L2-Norm

Figure 5: **(a)** and **(b)**: The relationship between noise reduction and transformation number. The surrogate models are trained on CIFAR-100 with rotation and resize-padding. The term "Current ASR / Best ASR" refers to the current attack success rate divided by the best attack success rate. **(c)** and **(d)**: The role of transformation number I and L2-norm.

4 Experiments

4.1 Experimental Setup

We describe the dataset, implementation setup, and input transformation setup in detail here.

Implementation Setup. Following the previous works Wang et al. (2021; 2023); Zhu et al. (2024a), we calculate attack success rate on 1,000 images chosen from ILSVRC 2012 validation set Russakovsky et al. (2015), and these images are classified correctly by all the models. Following the widely used hyperparameter setup in the works Dong et al. (2018); Zhu et al. (2024a); Lin et al. (2024), we set the perturbation budget ϵ to 16/255, iteration number T to 10, step size α to 1.6/255. By default, the transformation number I is 2,000. We run the experiments on a single A100.

Input Transformation Setup. The properties of a model may primarily depend on its structure, so we follow the experience shown in Fig. 4. By default, the input transformation set Ψ consists of block shuffle, resize-padding, SSM, random shift, random cropping, and random rotation. To expand the target function space, hyperparameters of input transformations are randomly selected as follows: Block-shuffle splits inputs into $1 \rightarrow 25$ randomly sized blocks; resize-padding adopts the configuration from Xie et al. (2019) with maximum scaling factor uniformly sampled from 1.14 to 1.66 (minimum fixed at 1.0); SSM applies noise factors sampled uniformly from 0.1 to 0.9; random shift magnitudes range from 0 to a predefined maximum; random cropping adds 0-30 pixels of padding before resizing to 224×224; and random rotation employs maximum angles uniformly distributed between 0 and 180.

4.2 Role of Hyperparameter and L2-Norm

We show the role of the transformation number I and L2-norm on our proposed SimAttack. The results are shown in Fig. 5. If the transformation number is too small, the gradient noise introduced by domain shifts may reduce performance.

4.3 Case Study on LLM

We take the ViT-B as the surrogate model and show the adversarial examples of SimAttack successfully attacking GPT 4.1 Achiam et al. (2023), as shown in Fig. 6. Large models still cannot escape the vulnerability of neural networks while people can still distinguish the images.

Prompt: Provide a concise description of the image using no more than three sentences.	
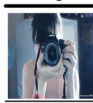	The image shows **a person holding a Canon camera and taking a photo**, with the camera covering most of their face. The background is softly blurred, and the lighting is cool-toned. The photo is credited to FiorellaLucia, 2008, in the bottom right corner.
	The image depicts **a close-up of an insect, possibly a beetle**, with a prominent circular structure on its back that resembles a camera lens. The insect is positioned on a smooth, light-colored surface. The overall appearance is surreal, blending biological and mechanical elements.
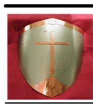	The image shows **a medieval-style shield** with a metallic surface and gold-colored trim. A gold cross is prominently featured in the center of the shield. The shield is displayed against a red background.
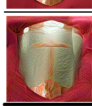	The image shows **a close-up view of a watermelon** with its rind partially exposed, surrounded by a reddish fabric. The lighting highlights the texture and pattern of the watermelon skin. The overall composition creates a colorful and somewhat abstract appearance.

Figure 6: Case study on GPT 4.1 examples.

4.4 Comparative Experiments

In this section, we adopt 5 common neural networks as surrogate models to compare our proposed AdaAES with other advanced attacks and evaluate the attack success rate of different transfer-based adversarial attacks on twelve models including ResNet18 He et al. (2016), ResNet50 He et al. (2016), ResNet101 He et al. (2016), ResNeXt50 Xie et al. (2017), DenseNet121 Huang et al. (2017), VGG19 Simonyan & Zisserman (2014), ViT-S Dosovitskiy et al. (2020), ViT-B Dosovitskiy et al. (2020), PiT-B Zhang et al. (2023), Visformer Chen et al. (2021), and Swin Transformer Liu et al. (2021). We pick 7 adversarial attacks (including MI-FGSM Dong et al. (2018), DEM Zou et al. (2020), SIA Wang et al. (2023), ANDA Fang et al. (2024), BSR Wang et al. (2024a), DeCowA Lin et al. (2024), L2T Zhu et al. (2024a), OPS Guo et al. (2025)) as the comparative methods. The results are shown in Tab. 2. The results show that our method outperforms all existing methods across multiple surrogate models, which supports the soundness of our work.

Table 2: Attack success rate (%) across twelve models on the adversarial examples crafted on a surrogate model (labeled “Sur.”).

Sur.	Attack	Res18	Res50	Res101	NeXt	Den	VGG	Incv3	ViT-S	ViT-B	PiT	Vis.	Swin	Mean
InceptionV3	MI-FGSM	47.3	30.0	28.1	28.5	44.5	47.9	97.9	23.1	13.7	16.9	24.3	28.8	35.9
	DEM	77.2	57.1	55.5	57.6	78.8	76.0	99.0	47.4	30.6	35.5	47.7	49.2	59.3
	SIA	87.9	69.2	65.4	69.0	85.9	83.6	99.9	49.1	34.7	46.5	58.9	61.5	67.6
	ANDA	66.1	50.1	48.4	49.8	69.5	66.0	99.7	38.1	27.2	31.8	42.9	45.6	52.9
	BSR	87.7	71.9	67.5	70.6	87.0	85.6	99.8	51.1	37.0	48.7	62.8	65.6	69.6
	DeCowA	78.7	57.8	57.3	61.1	78.5	78.8	98.0	47.4	32.1	38.9	49.6	54.7	61.1
	L2T	83.9	70.6	67.8	70.4	84.6	80.7	98.9	52.4	37.3	49.2	56.6	61.6	67.8
	OPS	96.2	83.6	85.1	85.5	95.9	91.9	99.9	77.3	59.9	65.4	77.9	80.7	83.3
	Ours	**98.2**	**92.3**	**91.8**	**93.3**	**98.1**	**98.0**	**100.0**	**82.9**	**71.0**	**77.3**	**87.3**	**87.8**	**89.8**
DenseNet121	MI-FGSM	74.9	61.5	50.9	55.2	99.9	68.5	58.0	31.6	20.6	27.9	41.4	44.3	52.9
	DEM	98.0	91.0	85.8	89.1	99.9	94.4	94.2	63.7	48.8	52.8	75.4	70.2	80.3
	SIA	98.6	95.6	92.2	94.9	**100.0**	97.6	91.9	64.6	48.3	67.5	84.6	81.7	84.8
	ANDA	93.4	86.2	81.0	83.6	99.9	89.8	82.6	53.7	40.8	55.3	71.0	69.8	75.6
	BSR	98.6	95.0	89.6	93.1	**100.0**	97.1	88.2	62.6	49.1	66.3	83.5	79.8	83.6
	DeCowA	98.5	92.5	89.0	91.4	**100.0**	96.4	93.8	73.3	57.7	70.3	83.4	80.6	85.6
	L2T	98.8	95.0	92.9	94.2	**100.0**	97.7	94.4	74.6	59.1	73.3	85.6	85.7	87.6
	OPS	99.9	98.2	98.5	98.3	**100.0**	98.7	99.2	90.6	79.8	86.0	94.7	93.4	94.8
	Ours	**100.0**	**99.9**	**99.7**	**99.7**	**100.0**	**99.8**	**99.7**	**94.0**	**85.2**	**91.0**	**97.4**	**96.6**	**96.9**
ResNet18	MI-FGSM	**100.0**	49.3	42.2	45.7	73.8	74.4	55.6	27.6	16.7	23.0	32.6	40.1	48.4
	DEM	**100.0**	82.5	76.8	81.8	97.5	95.1	92.1	58.7	39.1	46.0	66.3	65.9	75.2
	SIA	**100.0**	91.9	87.6	89.7	99.2	98.6	91.5	62.7	43.9	58.5	77.3	77.0	81.5
	ANDA	**100.0**	80.5	74.7	78.6	96.6	94.8	85.6	53.1	38.6	49.5	66.1	68.8	73.9
	BSR	**100.0**	90.5	86.0	88.4	98.8	98.7	90.3	60.8	43.0	57.9	77.3	75.9	80.6
	DeCowA	**100.0**	89.0	85.0	88.3	98.5	98.4	94.4	72.3	56.5	63.7	80.5	79.8	83.9
	L2T	**100.0**	91.5	87.6	91.6	98.6	98.8	94.8	67.4	51.0	64.7	78.8	81.2	83.8
	OPS	**100.0**	97.2	96.9	97.1	99.9	99.6	99.0	**91.4**	**77.1**	81.5	93.0	91.7	93.7
	Ours	**100.0**	**98.6**	**98.1**	**98.7**	**100.0**	**99.9**	**99.2**	90.6	76.5	**83.9**	**94.8**	**93.6**	**94.5**
ViT-S	MI-FGSM	51.4	33.6	30.3	33.8	48.9	54.7	45.0	**100.0**	69.2	37.4	42.6	54.1	50.1
	DEM	88.8	81.4	79.7	81.9	89.2	88.0	90.3	99.9	95.2	88.1	88.1	90.4	88.4
	SIA	86.2	80.3	76.4	78.3	87.4	85.8	80.6	**100.0**	95.7	84.9	86.0	90.3	86.0
	ANDA	70.7	60.8	57.4	60.8	73.3	71.0	67.4	**100.0**	89.1	67.5	69.7	77.1	72.1
	BSR	87.6	82.4	82.0	83.6	89.0	87.1	84.0	**100.0**	94.8	90.6	88.1	91.1	88.4
	DeCowA	86.0	75.7	73.8	77.5	97.1	85.3	84.2	98.8	87.2	83.4	83.6	85.9	84.9
	L2T	88.5	81.1	78.0	80.8	88.0	87.1	86.7	99.2	92.8	84.5	84.5	89.6	86.7
	OPS	96.1	91.1	93.0	92.8	96.6	94.2	97.2	99.7	97.0	95.0	95.2	96.0	95.3
	Ours	**98.1**	**95.7**	**96.0**	**97.3**	**98.5**	**97.6**	**98.3**	**100.0**	**98.9**	**98.1**	**98.3**	**98.8**	**98.0**
ViT-B	MI-FGSM	52.8	39.3	33.8	38.8	50.9	57.3	46.4	72.0	97.3	40.5	43.4	54.7	52.3
	DEM	85.1	77.8	78.5	78.4	87.4	85.3	86.3	93.7	97.9	86.9	85.2	85.9	85.7
	SIA	77.4	75.2	72.8	76.1	80.5	79.0	76.0	90.4	97.3	81.4	81.4	84.5	81.0
	ANDA	67.0	60.1	58.9	60.9	70.9	69.1	66.4	84.3	97.7	66.7	68.0	73.1	70.3
	BSR	74.9	73.7	71.7	73.2	78.4	75.2	75.3	84.1	93.9	78.2	76.0	79.7	77.9
	DeCowA	82.1	74.3	74.1	76.0	81.8	79.1	81.4	86.7	92.2	83.1	82.4	82.6	81.3
	L2T	82.9	78.2	76.7	77.9	83.0	82.3	82.0	90.2	95.7	82.2	82.6	85.5	83.3
	OPS	94.3	91.8	91.8	92.8	95.5	92.2	94.4	98.0	98.7	95.0	94.9	95.1	94.5
	Ours	**97.7**	**96.4**	**96.8**	**97.3**	**98.4**	**97.4**	**97.8**	**98.9**	**99.7**	**98.4**	**98.2**	**98.2**	**97.9**

5 CONCLUSIONS

This work reveals that: 1) To achieve model transformation-invariance, data transformations establish multiple projections from transformed inputs to outputs, rather than enabling models to capture invariant features during training. This suggests introducing the transformations into surrogate models. 2) Input transformation-based attacks leverage transformations to expand target function space, thereby improving adversarial transferability. The transform's ability to expand the function space may provide guidance across datasets. Also, normalization should be incorporated into the paradigm of the attacks due to gradient imbalance.

REFERENCES

Josh Achiam, Steven Adler, Sandhini Agarwal, Lama Ahmad, Ilge Akkaya, Florencia Leoni Aleman, Diogo Almeida, Janko Altenschmidt, Sam Altman, Shyamal Anadkat, et al. Gpt-4 technical report. *arXiv preprint arXiv:2303.08774*, 2023.

Bin Chen, Jiali Yin, Shukai Chen, Bohao Chen, and Ximeng Liu. An adaptive model ensemble adversarial attack for boosting adversarial transferability. In *Proceedings of the IEEE/CVF International Conference on Computer Vision*, pp. 4489–4498, 2023a.

Huanran Chen, Yichi Zhang, Yinpeng Dong, Xiao Yang, Hang Su, and Jun Zhu. Rethinking model ensemble in transfer-based adversarial attacks. *arXiv preprint arXiv:2303.09105*, 2023b.

Zhengsu Chen, Lingxi Xie, Jianwei Niu, Xuefeng Liu, Longhui Wei, and Qi Tian. Visformer: The vision-friendly transformer. In *Proceedings of the IEEE/CVF international conference on computer vision*, pp. 589–598, 2021.

Yinpeng Dong, Fangzhou Liao, Tianyu Pang, Hang Su, Jun Zhu, Xiaolin Hu, and Jianguo Li. Boosting adversarial attacks with momentum. In *Proceedings of the IEEE conference on computer vision and pattern recognition*, pp. 9185–9193, 2018.

Alexey Dosovitskiy, Lucas Beyer, Alexander Kolesnikov, Dirk Weissenborn, Xiaohua Zhai, Thomas Unterthiner, Mostafa Dehghani, Matthias Minderer, Georg Heigold, Sylvain Gelly, et al. An image is worth 16x16 words: Transformers for image recognition at scale. *arXiv preprint arXiv:2010.11929*, 2020.

Zhengwei Fang, Rui Wang, Tao Huang, and Liping Jing. Strong transferable adversarial attacks via ensembled asymptotically normal distribution learning. In *Proceedings of the IEEE/CVF Conference on Computer Vision and Pattern Recognition*, pp. 24841–24850, 2024.

Ian J Goodfellow, Jonathon Shlens, and Christian Szegedy. Explaining and harnessing adversarial examples. *arXiv preprint arXiv:1412.6572*, 2014.

Yu Guo, Weiquan Liu, Qingshan Xu, Shijun Zheng, Shujun Huang, Yu Zang, Siqi Shen, Chenglu Wen, and Cheng Wang. Boosting adversarial transferability through augmentation in hypothesis space. In *Proceedings of the Computer Vision and Pattern Recognition Conference*, pp. 19175–19185, 2025.

Kaiming He, Xiangyu Zhang, Shaoqing Ren, and Jian Sun. Deep residual learning for image recognition. In *Proceedings of the IEEE conference on computer vision and pattern recognition*, pp. 770–778, 2016.

Gao Huang, Zhuang Liu, Laurens Van Der Maaten, and Kilian Q Weinberger. Densely connected convolutional networks. In *Proceedings of the IEEE conference on computer vision and pattern recognition*, pp. 4700–4708, 2017.

Diederik P Kingma and Jimmy Ba. Adam: A method for stochastic optimization. *arXiv preprint arXiv:1412.6980*, 2014.

Alex Krizhevsky, Geoffrey Hinton, et al. Learning multiple layers of features from tiny images. Technical report, University of Toronto, 2009. URL `https://www.cs.toronto.edu/~kriz/cifar.html`.

Alexey Kurakin, Ian J Goodfellow, and Samy Bengio. Adversarial examples in the physical world. In *Artificial intelligence safety and security*, pp. 99–112. Chapman and Hall/CRC, 2018.

Qinliang Lin, Cheng Luo, Zenghao Niu, Xilin He, Weicheng Xie, Yuanbo Hou, Linlin Shen, and Siyang Song. Boosting adversarial transferability across model genus by deformation-constrained warping. In *Proceedings of the AAAI Conference on Artificial Intelligence*, volume 38, pp. 3459–3467, 2024.

Yanpei Liu, Xinyun Chen, Chang Liu, and Dawn Song. Delving into transferable adversarial examples and black-box attacks. *arXiv preprint arXiv:1611.02770*, 2016.

Ze Liu, Yutong Lin, Yue Cao, Han Hu, Yixuan Wei, Zheng Zhang, Stephen Lin, and Baining Guo. Swin transformer: Hierarchical vision transformer using shifted windows. In *Proceedings of the IEEE/CVF international conference on computer vision*, pp. 10012–10022, 2021.

Yuyang Long, Qilong Zhang, Boheng Zeng, Lianli Gao, Xianglong Liu, Jian Zhang, and Jingkuan Song. Frequency domain model augmentation for adversarial attack. In *European conference on computer vision*, pp. 549–566. Springer, 2022.

Ilya Loshchilov and Frank Hutter. Decoupled weight decay regularization. *arXiv preprint arXiv:1711.05101*, 2017.

Muhammad Muzammal Naseer, Salman H Khan, Muhammad Haris Khan, Fahad Shahbaz Khan, and Fatih Porikli. Cross-domain transferability of adversarial perturbations. *Advances in Neural Information Processing Systems*, 32, 2019.

Yunxiao Qin, Yuanhao Xiong, Jinfeng Yi, and Cho-Jui Hsieh. Training meta-surrogate model for transferable adversarial attack. In *Proceedings of the AAAI conference on artificial intelligence*, volume 37, pp. 9516–9524, 2023.

Olga Russakovsky, Jia Deng, Hao Su, Jonathan Krause, Sanjeev Satheesh, Sean Ma, Zhiheng Huang, Andrej Karpathy, Aditya Khosla, Michael Bernstein, et al. Imagenet large scale visual recognition challenge. *International journal of computer vision*, 115:211–252, 2015.

Ramprasaath R Selvaraju, Michael Cogswell, Abhishek Das, Ramakrishna Vedantam, Devi Parikh, and Dhruv Batra. Grad-cam: Visual explanations from deep networks via gradient-based localization. In *Proceedings of the IEEE international conference on computer vision*, pp. 618–626, 2017.

Karen Simonyan and Andrew Zisserman. Very deep convolutional networks for large-scale image recognition. *arXiv preprint arXiv:1409.1556*, 2014.

Kunyu Wang, Xuanran He, Wenxuan Wang, and Xiaosen Wang. Boosting adversarial transferability by block shuffle and rotation. In *Proceedings of the IEEE/CVF Conference on Computer Vision and Pattern Recognition*, pp. 24336–24346, 2024a.

Ruikui Wang, Yuanfang Guo, and Yunhong Wang. Ags: Affordable and generalizable substitute training for transferable adversarial attack. In *Proceedings of the AAAI Conference on Artificial Intelligence*, volume 38, pp. 5553–5562, 2024b.

Xiaosen Wang, Xuanran He, Jingdong Wang, and Kun He. Admix: Enhancing the transferability of adversarial attacks. In *Proceedings of the IEEE/CVF International Conference on Computer Vision*, pp. 16158–16167, 2021.

Xiaosen Wang, Zeliang Zhang, and Jianping Zhang. Structure invariant transformation for better adversarial transferability. In *Proceedings of the IEEE/CVF International Conference on Computer Vision*, pp. 4607–4619, 2023.

Dongxian Wu, Yisen Wang, Shu-Tao Xia, James Bailey, and Xingjun Ma. Skip connections matter: On the transferability of adversarial examples generated with resnets. *arXiv preprint arXiv:2002.05990*, 2020.

Wang Xiaosen, Kangheng Tong, and Kun He. Rethinking the backward propagation for adversarial transferability. *Advances in Neural Information Processing Systems*, 36:1905–1922, 2023.

Cihang Xie, Zhishuai Zhang, Yuyin Zhou, Song Bai, Jianyu Wang, Zhou Ren, and Alan L Yuille. Improving transferability of adversarial examples with input diversity. In *Proceedings of the IEEE/CVF conference on computer vision and pattern recognition*, pp. 2730–2739, 2019.

Saining Xie, Ross Girshick, Piotr Dollár, Zhuowen Tu, and Kaiming He. Aggregated residual transformations for deep neural networks. In *Proceedings of the IEEE conference on computer vision and pattern recognition*, pp. 1492–1500, 2017.

Shawn Xu, Subhashini Venugopalan, and Mukund Sundararajan. Attribution in scale and space. In *Proceedings of the IEEE/CVF Conference on Computer Vision and Pattern Recognition*, pp. 9680–9689, 2020.

Jianping Zhang, Yizhan Huang, Weibin Wu, and Michael R Lyu. Transferable adversarial attacks on vision transformers with token gradient regularization. In *Proceedings of the IEEE/CVF Conference on Computer Vision and Pattern Recognition*, pp. 16415–16424, 2023.

Bolei Zhou, Aditya Khosla, Agata Lapedriza, Aude Oliva, and Antonio Torralba. Learning deep features for discriminative localization. In *Proceedings of the IEEE conference on computer vision and pattern recognition*, pp. 2921–2929, 2016.

Rongyi Zhu, Zeliang Zhang, Susan Liang, Zhuo Liu, and Chenliang Xu. Learning to transform dynamically for better adversarial transferability. In *Proceedings of the IEEE/CVF Conference on Computer Vision and Pattern Recognition*, pp. 24273–24283, 2024a.

Zhiyu Zhu, Huaming Chen, Xinyi Wang, Jiayu Zhang, Zhibo Jin, Kim-Kwang Raymond Choo, Jun Shen, and Dong Yuan. Ge-advgan: Improving the transferability of adversarial samples by gradient editing-based adversarial generative model. In *Proceedings of the 2024 SIAM International Conference on Data Mining (SDM)*, pp. 706–714. SIAM, 2024b.

Yue Zhuo and Zhiqiang Ge. Ig 2: Integrated gradient on iterative gradient path for feature attribution. *IEEE Transactions on Pattern Analysis and Machine Intelligence*, 46(11):7173–7190, 2024.

Junhua Zou, Zhisong Pan, Junyang Qiu, Xin Liu, Ting Rui, and Wei Li. Improving the transferability of adversarial examples with resized-diverse-inputs, diversity-ensemble and region fitting. In *European Conference on Computer Vision*, pp. 563–579. Springer, 2020.

A Appendix

A.1 Ablation Study on Input Transformation

By default, the input transformation set Ψ employed by our proposed SimAttack consists of block shuffle, resize-padding, SSM, random shift, random cropping, and random rotation. We further demonstrate the impact of adding and removing input transformations on our proposed SimAttack, as shown in Tabs. 3 and 4. The results supports that the selected transformation is the best setup.

Table 3: Attack success rate (%) across twelve models on the adversarial examples crafted on ResNet18 by our proposed SimAttack with different transformations. By default, the input transformation set Ψ employed by our proposed SimAttack consists of block shuffle, resize-padding, SSM, random shift, random cropping, and random rotation.

Method	Res18	Res50	Res101	NeXt	Den	VGG	Incv3	ViT-S	ViT-B	PiT	Vis.	Swin	Mean
- Random shift	100	97.8	96.7	97.6	100	99.9	98.9	89.2	73.0	81.9	93.1	92.4	93.4
SimAttack (Ours)	100	98.6	98.1	98.7	100	99.9	99.2	90.6	76.5	83.9	94.8	93.6	94.5
+ Gaussian blurring	100	97.4	96.6	97.5	100	99.8	98.5	89.2	73.3	81.3	92.6	90.9	93.1
+ Dropout	100	97.0	95.5	96.8	99.9	99.9	98.5	88.5	71.2	79.8	92.7	90.7	92.5
+ Random scaling	100	96.5	95.7	96.6	99.9	99.4	98.5	87.5	70.8	78.6	92.1	90.2	92.2
+ Random Flip	100	97.4	96.7	97.4	99.9	99.5	98.8	89.2	73.2	80.3	92.3	91.6	93.0

Table 4: Attack success rate (%) across twelve models on the adversarial examples crafted on ViT-S by our proposed SimAttack with different transformations. By default, the input transformation set Ψ employed by our proposed SimAttack consists of block shuffle, resize-padding, SSM, random shift, random cropping, and random rotation.

Method	Res18	Res50	Res101	NeXt	Den	VGG	Incv3	ViT-S	ViT-B	PiT	Vis.	Swin	Mean
- Random shift	98.2	95.3	96.2	96.7	98.3	97.6	98.5	100	98.8	97.8	98.1	99.0	97.9
SimAttack (Ours)	98.1	95.9	96.1	97.2	98.5	97.6	98.3	100	98.9	98.1	98.4	98.8	98.0
+ Gaussian blurring	97.6	93.3	93.5	95.3	98.5	96.1	97.4	100	98.5	97.6	96.5	98.1	96.9
+ Dropout	97.2	93.0	92.8	94.5	98.1	96.0	97.0	100	98.6	97.1	96.3	98.0	96.6
+ Random scaling	97.2	91.5	92.1	93.1	97.5	95.6	96.3	100	98.3	96.7	95.5	97.2	95.9
+ Random Flip	97.3	92.0	91.8	93.6	97.3	95.8	96.8	100	98.4	96.5	95.7	97.1	96.0

A.2 Case Study on LLM

We take 5 neural networks (i.e., DenseNet18, InceptionV3, ResNet18, ViT-S and ViT-B) as the surrogate models, respectively, and show the adversarial examples of SimAttack successfully attacking GPT 4.1, as shown in Figs. 7 and 8. The surrogate models are trained on ImageNet dataset. Overall, large models still cannot escape the vulnerability of neural networks while people can still distinguish the images. In Addition, the results in Row 1 (right) suggests that the two models based on the transform structure may be more effective than convolutional neural networks (CNNs) in attacking large language models, since the adversarial examples generated by ViT-S and ViT-B successfully attack the GPT 4.1 but the ones generated by DenseNet121, InceptionV3 and ResNet18 are unable to do so.

A.3 The Use of Large Language Models

We employ large language models to check for typos and grammatical errors, and utilize the LLMs to provide suggestions for fixing code bugs.

Prompt: Provide a concise description of the image using no more than three sentences.

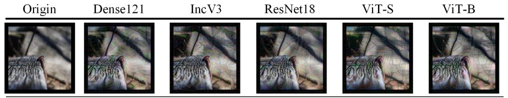

Origin	Dense121	IncV3	ResNet18	ViT-S	ViT-B
The image shows a close-up of a rusty nail partially embedded in a piece of weathered wood. The nail is bent, and the background is blurred, emphasizing the texture of the wood and the nail. The lighting creates a strong contrast between the foreground and background.	The image appears to be an abstract or heavily stylized depiction of an animal, possibly a cat, with visible fur textures and an ear. The colors are muted, with a mix of greens, browns, and grays, giving it a dreamy or surreal effect. The overall composition is somewhat blurry, making it difficult to clearly Dropoutntify specific details.	The image depicts the back of a white animal, likely a tiger, with distinct black stripes and a visible ear. The scene is overlaid with a dreamy, abstract pattern that gives it a surreal appearance. The overall color palette is muted, with soft blending of light and shadow.	The image shows the back of a white tiger's head, with distinct black stripes and a visible ear. The scene is overlaid with a subtle, abstract pattern resembling leaves or veins. The overall appearance is slightly surreal due to the blending of natural and abstract elements.	The image appears to show the back of a white tiger's head with black stripes, partially obscured by shadows and branches. The perspective seems to be from behind the animal, focusing on its ear and fur pattern. The overall image has a slightly abstract or filtered effect.	The image shows a close-up view of an animal, likely a cat, focusing on its ear and the surrounding fur. The background is blurred, with some branches or lines visible. The overall effect is somewhat abstract, with muted colors and soft textures.

Prompt: Provide a concise description of the image using no more than three sentences.

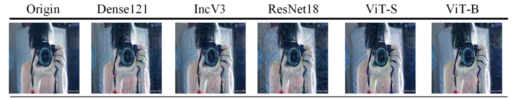

Origin	Dense121	IncV3	ResNet18	ViT-S	ViT-B
The image shows a person holding a Canon camera and taking a photo, with the camera covering most of their face. The background is softly blurred, and the lighting is cool-toned. The photo is credited to FiorellaLucia, 2008, in the bottom right corner.	The image shows a surreal, dream-like rendering of a person holding a camera up to their face. The scene is heavily stylized, with blended colors and textures that give it an abstract appearance. The word "Canon" is faintly visible on the camera, suggesting the brand.	The image shows a person holding a camera up to their face, taking a photo or self-portrait. The image is heavily stylized with a wavy, textured effect, giving it an abstract appearance. The camera brand "Canon" is visible on the lens.	The image depicts a person holding a camera up to their face, appearing to take a photograph. The scene is rendered in a painterly, textured style with cool blue and white tones dominating the palette. The camera brand "Canon" is visible, and the overall effect is abstract and artistic.	The image appears to be an abstract or heavily stylized depiction of a fish placed on a surface, possibly a table. The colors are muted with a bluish tint, and some details are distorted, making it look surreal or dreamlike. The central focus is on the fish's head and mouth area, with some digital effects present.	The image depicts a close-up of an insect, possibly a beetle, with a prominent circular structure on its back that resembles a camera lens. The insect is positioned on a smooth, light-colored surface. The overall appearance is surreal, blending biological and mechanical elements.

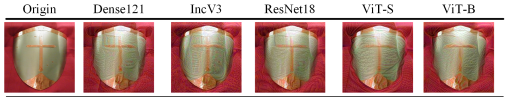

Origin	Dense121	IncV3	ResNet18	ViT-S	ViT-B
The image shows a medieval-style shield with a metallic surface and gold-colored trim. A gold cross is prominently featured in the center of the shield. The shield is displayed against a red background.	The image depicts an abstract, stylized rendering of a medieval knight’s helmet, set against a red textured background. The colors are blended and wavy, giving the image a surreal, dream-like quality. Details on the helmet are softened, making it appear almost as if it is melting or part of a painting.	The image shows a shiny, irDropoutscent shell placed on a red textured cloth background. The shell has a smooth surface with green, pink, and orange hues. Its shape is somewhat oval with a pointed end at the bottom.	The image features a central, helmet-like object with a pale, textured surface and subtle cross-shaped markings. The background is a vivid red with swirling patterns, creating a striking contrast with the central figure. The overall appearance is abstract and artistic, with an emphasis on texture and color blending.	The image shows a close-up of a pale, textured object that resembles a peeled fruit or vegetable, possibly an orange or grapefruit segment. The background is a vivid reddish-pink fabric, adding contrast to the central object. The overall effect is somewhat abstract due to the unusual lighting and color blending.	The image shows a close-up view of a watermelon with its rind partially exposed, surrounded by a reddish fabric. The lighting highlights the texture and pattern of the watermelon skin. The overall composition creates a colorful and somewhat abstract appearance.

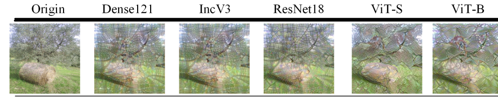

Origin	Dense121	IncV3	ResNet18	ViT-S	ViT-B
The image shows a large round hay bale resting on green grass in front of a leafy tree. The scene is outdoors, likely in a rural or agricultural area. The lighting is natural, and the setting appears peaceful and calm.	The image shows a close-up view of a spDropoutr web with dew drops glistening in the sunlight. The web is intricately woven and appears to be outdoors, with green foliage visible in the background. The overall effect creates a shimmering, almost abstract pattern.	The image shows a close-up view of a spDropoutr web with droplets of water on it. The web appears to be outdoors, with greenery and blurred natural background visible through the delicate threads. The light reflecting off the water droplets creates a shimmering effect across the web.	The image features a snake camouflaged among green foliage, blending into its natural surroundings. The overall appearance is distorted with a grid-like, dreamlike texture overlay, making the scene look surreal. The snake's head and body are faintly visible through the abstract effects.	The image shows a close-up view of a rock surface covered with patches of green moss and lichen. The rocks have a rough, uneven texture and are various shades of brown and gray. The overall scene appears natural and outdoors.	The image shows a chameleon blending into its leafy surroundings, camouflaged among green branches and foliage. The scene is overlaid with a textured, almost mosaic-like artistic effect. The overall appearance is abstract, making the chameleon subtly integrated into the background.

Figure 7: Case study on GPT 4.1 examples.

Prompt: Provide a concise description of the image using no more than three sentences.

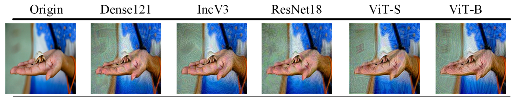

Origin	Dense121	IncV3	ResNet18	ViT-S	ViT-B
A person is holding a small hermit crab in their open palm. The background is out of focus, highlighting the crab and the hand. The person is wearing a blue and white outfit with an orange bracelet on their wrist.	The image shows a surreal, digitally altered depiction of a bat or similar animal with outstretched wings and a distorted face. The background is a blend of blue and green hues with a textured, dreamlike appearance. The overall effect is artistic and abstract, making the subject appear otherworldly.	The image shows a hand gently holding a small butterfly or moth, with a surreal, artistic filter applied. The background features blue and green hues with a dreamy, textured effect. The overall style gives the scene an abstract and otherworldly appearance.	The image appears to be a surreal, digitally manipulated artwork showing a hand holding a butterfly. The hand and surrounding area are rendered in a painterly, dreamlike style with swirling textures and vibrant colors. The overall effect is abstract and imaginative, blending reality with fantasy.	This image depicts a surreal, digitally altered hand holding a butterfly, rendered in a painterly, abstract style. The background features swirling textures in green and blue tones, giving it a dreamlike quality. The overall composition blends realistic elements with imaginative, artistic effects.	The image appears to be an abstract or heavily stylized depiction of an animal with a long snout, possibly resembling an anteater or a similar creature. The colors are vivid and the textures are distorted, giving the image a dreamlike or surreal quality. The background features blue and green hues, further enhancing the surreal effect.

Prompt: Provide a concise description of the image using no more than three sentences.

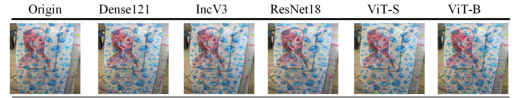

Origin	Dense121	IncV3	ResNet18	ViT-S	ViT-B
The image shows a sheet or curtain decorated with blue sea-themed patterns such as shells, starfish, and fish. Over these patterns, there is a red, sketchy drawing of a person with large eyes and a somber expression. The setting appears to be indoors, possibly in an art studio or installation space.	The image appears to be an abstract or computer-generated artwork with layered, distorted shapes and patterns. Blue fish-like figures and pinkish swirls dominate the composition, giving it a surreal, dreamlike quality. The overall effect is visually complex and somewhat disorienting.	This image features a surreal, abstract design with a pinkish, face-like figure near the top left. The background is filled with repeated blue fish shapes and various geometric patterns. The overall appearance is dreamlike and digitally manipulated.	This image displays a digitally altered, abstract scene featuring a pinkish, humanoid figure in the upper left. The background is filled with repetitive blue shapes resembling fish or leaves, creating a surreal, dreamlike effect. The overall composition is complex and visually distorted.	This image features a surreal, abstract design with a central pinkish cluster that resembles flowers or a bouquet. The background is filled with repetitive blue shapes, possibly stylized leaves or fish, set against a soft, pastel backdrop. The overall effect is dreamlike and visually complex.	The image shows a colorful, patterned jacket and pants set laid out flat, with a pink and blue tie-dye design. There is a bouquet of artificial flowers placed on top of the jacket. The background appears to be a textured surface, possibly a rug or blanket.

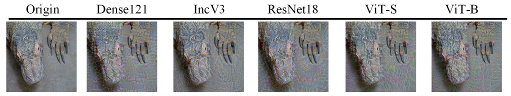

Origin	Dense121	IncV3	ResNet18	ViT-S	ViT-B
The image shows a close-up of a Komodo dragon lying on the ground. Its textured, scaly face and large, clawed forelimb are prominently visible. The Komodo dragon appears calm and relaxed.	The image appears to be heavily stylized or processed, possibly with a neural network filter, giving it a dreamlike and abstract quality. There is a faint outline of what looks like a hand with visible fingers on the right side. The background is textured and puzzle-like, making it difficult to clearly distinguish specific objects.	The image shows a surreal, dreamlike rendering of what appears to be an animal's limb and paw, possibly a reptile or lizard. The surface is covered with intricate, lace-like patterns that give it an artificial or stylized look. The background is plain and does not distract from the main subject.	The image depicts a textured, abstract rendering of what appears to be an animal limb with visible claws or talons. The surface is rough and patterned, giving a surreal, artistic effect. The background is muted and does not distract from the main subject.	The image shows an abstract, textured depiction of an animal limb with several long, curved claws. The background is soft and multicolored, creating a dreamy effect. The limb appears rough and patterned, drawing focus to the distinct claws.	The image appears to show a textured, woolly object hanging on a wall, possibly a handmade craft or decoration. There are also several small objects or charms dangling next to it, resembling a dreamcatcher or similar ornament. The colors are muted with a pastel overlay, giving the image an artistic, almost painted effect.

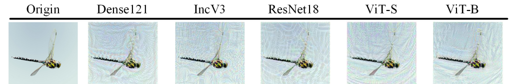

Origin	Dense121	IncV3	ResNet18	ViT-S	ViT-B
The image shows a dragonfly in flight against a plain, light blue background. The dragonfly has transparent wings and a long, segmented body with yellow and black markings. The details of its wings and body are clearly visible.	The image appears to be an abstract or stylized depiction of an object with a long, serrated edge, possibly resembling a saw or a swordfish's bill. The background is textured with swirling, pastel-like patterns. The central object is metallic with some yellow and black coloring.	The image shows a stylized or abstract depiction of an insect, likely a dragonfly, with a segmented body and transparent wings. The background is textured with light pastel patterns, giving the image an artistic effect. The main colors of the insect are yellow, black, and metallic shades.	The image features an abstract or stylized depiction of a dragonfly with translucent wings and a segmented, dark-colored body. The background has a light, web-like texture that adds an artistic effect. The dragonfly's body displays yellow and black markings.	The image shows a stylized or abstract representation of a dragonfly with a long, segmented body and transparent wings. The background is light and textured, giving a soft, artistic effect. The dragonfly features yellow and black markings on its body.	The image depicts a long, segmented object resembling a fish or aquatic creature with a paddle-like tail, suspended against a light, textured background. The colors and patterns are somewhat surreal and digitally altered, giving the scene an artistic, dreamlike quality. The overall composition is minimalistic, with the main subject positioned off-center.

Figure 8: Case study on GPT 4.1 examples.